Nonlinear Alfvén, magnetosonic, sound, and electron inertial waves in fluid formalism

K. Stasiewicz[1]

Swedish Institute of Space Physics, Uppsala, Sweden

Received 20 October 2004; revised 17 December 2004; accepted 22 December 2004; published 29 March 2005.

[1] A fluid model of nonlinear electron and ion inertial waves in anisotropic plasmas is presented. The model has been verified for plasma beta (ratio of kinetic/magnetic pressures) in a range between 0.1 and 15. It is shown that warm plasmas support four types of nonlinear waves, which correspond to four linear modes, Alfvénic, magnetosonic, sound, and electron inertial waves. Each of these nonlinear modes has slow and fast versions. Modes slower than the sound speed have left-handed polarization for the transverse magnetic field, while the faster modes have right-handed polarization. It is shown by direct integration that the exponential growth rate of nonlinear modes is balanced by the ion and electron dispersion leading to solutions in the form of trains of solitons or cnoidal waves. By using a novel technique of phase portraits, it is shown how the dispersive properties of electron and ion inertial waves change at the transition between warm and hot plasmas ($\beta \approx 1$) and how trains of solitons (''mirror modes'') are produced in a hot, anisotropic plasma. The applicability of the model is illustrated by showing that the electric currents carried by nonlinear waves measured on Cluster spacecraft in the magnetosheath at $\beta \approx 15$ are well reproduced by currents derived from the theoretical model.

Citation: Stasiewicz, K. (2005), Nonlinear Alfvén, magnetosonic, sound, and electron inertial waves in fluid formalism, *J. Geophys. Res.*, *110*, A03220, doi:10.1029/2004JA010852.

1. Introduction

[2] The magnetohydrodynamic (MHD) waves, first theoretically predicted by *Alfvén* [1942], have been the subjects of numerous studies and publications. They are known to describe the dynamics of low-frequency electromagnetic phenomena in the terrestrial magnetosphere, on the Sun, and in astrophysical plasmas. These waves interact strongly both with ions and electrons, which leads to direct acceleration and heating of particles in space and laboratory plasmas and to indirect effects on high-energy particles scattered on Alfvénic turbulence. The first models based on ideal MHD equations have been extended by including dispersive effects related to ion and electron inertia (represented by inertial lengths $\lambda_i = c/\omega_{pi}$ and $\lambda_e = c/\omega_{pe}$), kinetic effects related to finite thermal ion gyroradius ($r_B = v_{ti}/\omega_{ci}$) and finite plasma beta, and to inhomogeneity of the background plasma (see, for example, *Braginski* [1965], *Stringer* [1963], *Formisano and Kennel* [1969], and many others). Here, ω_{pe} and ω_{pi} denote electron and ion plasma frequencies, ω_{ci} is the ion gyrofrequency, v_{ti} is the ion thermal speed, and c is the speed of light. The electron and ion beta are defined as $\beta_j = 2\mu_0 p_j/B^2$, where p_j is the kinetic pressure for particle species ''j.''

[3] Recently, a great deal of attention was devoted to dispersive effects of Alfvén waves related to the electron inertial length λ_e, which ranges from around 50 m in the topside ionosphere to several kilometers in the magnetosphere. Works of *Stefant* [1970], *Hasegawa* [1976], and *Goertz and Boswell* [1979] stimulated many papers dealing with applications of dispersive Alfvén waves to auroral physics. It is now believed that electron inertial waves can create nonlinear structures responsible for discrete auroral arcs with thickness of $\sim$100 m (see, for example, the review by *Stasiewicz et al.* [2000]).

[4] The dispersive properties of both electron inertial and kinetic Alfvén waves have been measured in laboratory experiments by *Gekelman et al.* [2000] and *Vincena et al.* [2004]. The electron scale dispersion is important for perpendicular propagation of Alfvén waves in cold plasmas $\beta_e \sim \beta_i < m_e/m_i$, which implies r_s, $r_B < \lambda_e$, while in the opposite limit the dispersion related with finite thermal ion gyroradius r_B and ion acoustic gyroradius r_s (ion gyroradius at the electron temperature) becomes increasingly important. In addition to the ion gyroradius effects, the kinetic limit $\beta_e > m_e/m_i$ implies $v_{te} > V_A$ (the Alfvén speed), which means that the fast-moving thermal electrons are able to respond adiabatically to the presence of the wave fields, while in the cold limit one expects effects related to electron inertia, e.g., a parallel electric field.

[5] Generally, the ion inertia terms ($\propto k\lambda_i$) are larger than the electron inertia terms by a factor $(m_i/m_e)^{1/2} \gtrsim 43$ and should dominate the electron effects in most circumstances

[1] Also at Space Research Centre, Polish Academy of Sciences, Warsaw, Poland.

Copyright 2005 by the American Geophysical Union.
0148-0227/05/2004JA010852$09.00

(here, $k = 2\pi/\lambda$ is the wave number). Indeed, the ion inertia terms are found to be responsible for creation of solitons and other nonlinear structures observed in planetary magnetospheres and around comets, as has been recently elaborated in a series of articles by *Baumgärtel* [1999], *Sauer et al.* [2003], *McKenzie et al.* [2003], and *Dubinin et al.* [2003], following earlier fully nonlinear analyzes of *Hau and Sonnerup* [1991].

[6] Using Cluster measurements, *Stasiewicz et al.* [2003b] and *Stasiewicz* [2004a, 2004b] have shown that the Hall-MHD equations which include ion inertia effects provide good quantitative description of large amplitude waves, solitons, and mirror modes in high-beta plasmas of the magnetosheath and the boundary layers ($\beta \sim 0.1$–10). Such results justify the application of fluid equations to warm and hot plasmas, where kinetic effects are included through finite pressure of electrons and ions and by pressure anisotropy.

[7] In this paper, we present a systematic and detailed analysis of nonlinear effects related to magnetohydrodynamic modes in warm and hot anisotropic plasmas. Because of the ambiguous and confusing nomenclature of low-frequency wave modes encountered in the literature, this paper has some tutorial elements with basic equations and illustrations aimed to clarify the classification and identification of linear and nonlinear hydromagnetic waves. Furthermore, by including ion and electron inertia, low and high beta, isotropic and anisotropic plasma, we will be able to identify the importance of these effects in the parameter space for both linear and nonlinear waves. Cluster measurements are used to illustrate the general applicability of the fluid model to hot and anisotropic plasmas ($\beta \sim 10$), which are frequently encountered in space measurements.

2. Theory

2.1. Nonlinear Two-Fluid Model

[8] Computation of the first two moments of the Vlasov equation for a collisionless plasma consisting of electrons and ions leads to equations of continuity

$$\partial_t N_j + \nabla \cdot \left(N_j \mathbf{V}_j\right) = 0, \tag{1}$$

and momentum conservation

$$N_j m_j \frac{\mathrm{d}\mathbf{V}_j}{\mathrm{d}t} = N_j q_j \left(\mathbf{E} + \mathbf{V}_\mathrm{j} \times \mathbf{B}\right) - \nabla \cdot \mathbf{P}_j, \tag{2}$$

where "j" denotes particle species with number density N_j, mass m_j, charge q_j, velocity $\mathbf{V}_j$, and pressure $\mathbf{P}_j$. The electric and magnetic fields are denoted by $\mathbf{E}$ and $\mathbf{B}$, respectively. Summation of the electron and ion equations (2) leads to the momentum equation for the center of mass velocity, which is practically the ion flow velocity $\mathbf{V}$

$$N m_i (\partial_t \mathbf{V} + V_x \partial_x \mathbf{V}) = \mathbf{J} \times \mathbf{B} - \partial_x \mathbf{P}, \tag{3}$$

while another summation of (2), after multiplying both sides by q_j/m_j, leads to the generalized Ohm's law for the electric current $\mathbf{J}$

$$\frac{m_e}{Ne^2}\left[\partial_t \mathbf{J} + \partial_x (V_x \mathbf{J})\right] + \frac{1}{Ne}(\mathbf{J} \times \mathbf{B} - \partial_x \mathbf{p}_e) = \mathbf{E} + \mathbf{V} \times \mathbf{B}. \tag{4}$$

In the above equations we assumed quasi-neutrality, $N_i = N_e = N$, and one-dimensional propagation along the x axis. The pressure tensor (for electrons + ions) is

$$P_{kl} = p_\perp \delta_{kk} + \left(p_\parallel - p_\perp\right)\hat{b}_k \hat{b}_l, \tag{5}$$

where $\hat{b}_k$ are components of the unit vector $\mathbf{B}/B$. We assume a general relation for the perpendicular pressure

$$p_\perp = p_{\perp 0}(N/N_0)^\gamma (B/B_0)^\kappa \tag{6}$$

(where subscripts "0" denote background values) and define the pressure anisotropy parameter

$$a_p = p_\parallel / p_\perp - 1, \tag{7}$$

which generally may depend on N and B. The electron pressure in (4) is assumed to be isotropic and polytropic, $p_e = \propto N^{\gamma_e}$.

[9] Nonlinear waves, as well as linear ones, are conveniently studied in the stationary wave frame by the substitution $x \mapsto x + V_f t$ because the problem becomes time-independent and curl$\mathbf{E} = -\partial\mathbf{B}/\partial t = \mathbf{0}$ in this frame. In the wave frame plasma is moving in the x direction, at an angle α to $\mathbf{B}_0 = B_0(\cos\alpha, 0, \sin\alpha)$ with velocity (V_{x0}, 0, 0) = $V_f = \omega/k$ at $x = -\infty$ and the background density N_0. The magnetic field component $B_x = const$ (because $\nabla \cdot \mathbf{B} = 0$), and the continuity equation leads to flux conservation, $NV_x = const$. The x component of the momentum equation (3) can be integrated, and in dimensionless form ($\mathbf{b} = \mathbf{B}/B_0$, $V_{x0}/V_x = N/N_0 = n$) becomes

$$\begin{aligned} &2M^2\left(n^{-1} - 1\right) + \beta(n^\gamma b^\kappa - 1) + \left(b^2 - 1\right) \\ &\quad + \beta a_p \left(n^\gamma b^{\kappa-2} - 1\right)\cos^2\alpha = 0, \end{aligned} \tag{8}$$

where $\beta = 2\mu_0 p_{\perp 0}/B_0^2$, $M^2 = V_f^2/V_A^2$ is the square of the Alfvén Mach number and $V_A^2 = B_0^2/\mu_0 N_0 m_i$. The four terms in the above equation represent dynamic, kinetic, magnetic, and anisotropic kinetic pressures.

[10] Expressing lengths in units of $\lambda_i = V_A/\omega_{ci}$, $x \mapsto x\lambda_i$, we can write the transverse components of the generalized Ohm's law (4) in the following form

$$\begin{aligned} &-R\,\partial_x\left(n^{-1}\partial_x b_z\right) + M_\alpha^{-1}\partial_x b_y = \sin\alpha\left[n - \frac{n}{M_\alpha^2}\left(1 - \frac{\beta}{2}a_p\right)\right] \\ &- b_z\left[1 - \frac{n}{M_\alpha^2}\left(1 - \frac{\beta}{2}a_p n^\gamma b^{\kappa-2}\right)\right], \end{aligned} \tag{9}$$

$$R\,\partial_x\left(n^{-1}\partial_x b_y\right) + M_\alpha^{-1}\partial_x b_z = b_y\left[1 - \frac{n}{M_\alpha^2}\left(1 - \frac{\beta}{2}a_p n^\gamma b^{\kappa-2}\right)\right], \tag{10}$$

where $M_\alpha = M/\cos\alpha$ and $R = m_e/m_i$. Equations (8)–(10) form a complete system of equations for the spatial dependence of the field variables n, b_y, and b_z (and other derivables, such as flows, currents, and electric fields) in terms of the parameters M, β, α, γ, κ, and a_p. They are

fully nonlinear and equivalent to the original set of equations (3)–(7). In the limit of negligible electron inertia, $R = 0$, they correspond to equations derived by *Stasiewicz* [2004a].

[11] Using the normalizations that unit length is λ_i, velocity is V_A, current is $B_0/\mu_0\lambda_i$, and electric field is $V_A B_0$, we can express the other field quantities in normalized form in the plasma frame

$$v_x = M\left(n^{-1} - 1\right) \tag{11}$$

$$v_y = \frac{b_y}{M_\alpha}\left(1 - \frac{\beta}{2}a_p n^\gamma b^{\kappa-2}\right) \tag{12}$$

$$v_z = \frac{b_z}{M_\alpha}\left(1 - \frac{\beta}{2}a_p n^\gamma b^{\kappa-2}\right) - \frac{\sin\alpha}{M_\alpha}\left(1 - \frac{\beta}{2}a_p\right) \tag{13}$$

$$j_y = -\partial_x b_z \tag{14}$$

$$j_z = \partial_x b_y \tag{15}$$

$$e_x = v_z b_y - v_y b_z - n^{-1}\left(b_y\partial_x b_y + b_z\partial_x b_z\right) - \frac{\beta_e}{2}\gamma_e n^{\gamma_e - 2}\partial_x n \tag{16}$$

$$e_y = M\left(\sin\alpha - n^{-1}b_z\right) \tag{17}$$

$$e_z = Mn^{-1}b_y. \tag{18}$$

In this frame all quantities are zero at $x = -\infty$, where $\mathbf{b}_0 = (\cos\theta, 0, \sin\theta)$ and $n = 1$.

[12] The pressure anisotropy parameter $a_p(n, b)$ can have arbitrary functional form in (8)–(18). In what follows, we assume that the anisotropy parameter is constant. This assumption is consistent with previous works, which have established that the pressure anisotropy in the magnetosheath is a weak function of plasma β and that instabilities keep the ion anisotropy at nearly constant, marginal stability level [*Anderson et al.*, 1994; *Gary et al.*, 1994; *Denton et al.*, 1995].

[13] Equation (8) determines general interdependence between the density n and the magnetic field b, implied by conservation of momentum. It should hold for structures with arbitrary large amplitudes, also with kinetic effects, providing there is no strong nonlocal dissipation of energy by, e.g., large gyroradius ions. A discussion of this equation and representative plots in different plasma regimes can be found in the work of *Stasiewicz* [2004a]. Equation (8) implies the following relation between n and b:

$$\frac{\partial n}{\partial b} = \frac{2b + \beta n^\gamma b^{\kappa-1}\left[\kappa + (\kappa-2)a_p b^{-2}\cos^2\alpha\right]}{2M^2 n^{-2} - \beta\gamma n^{\gamma-1}b^\kappa\left(1 + a_p b^{-2}\cos^2\alpha\right)}, \tag{19}$$

which will be used in the next section to linearize the governing equations.

2.2. Linearization

[14] Equations (8)–(10) can be linearized around the background state, $n = 1 + \delta n$, $b_y = 0 + \delta b_y$, $b_z = b_{z0} + \delta b_z$, and the behavior of small amplitude waves determined by seeking exponentially varying solutions $\propto \exp(\pm kx)$. This procedure leads to the general dispersion equation for linear and nonlinear MHD modes that include ion and electron inertia effects, finite plasma beta, and pressure anisotropy

$$K^4M^2R^2 - K^2\left[R(2A - C) - \cos^2\alpha\right] + M^{-2}A(A - C) = 0, \tag{20}$$

where

$$A = M^2 - \left(1 - \frac{\beta}{2}a_p\right)\cos^2\alpha, \tag{21}$$

$$C = \left(M^2 - \frac{\beta}{2}\gamma a_p\cos^2\alpha\right)D\sin^2\alpha - \frac{\beta}{2}(\kappa - 2)a_p\cos^2\alpha\sin^2\alpha, \tag{22}$$

$$D = \left(\frac{\partial n}{\partial b}\right)_0 = \frac{2 + \kappa\beta + (\kappa-2)\beta a_p\cos^2\alpha}{2M^2 - \beta\gamma\left(1 + a_p\cos^2\alpha\right)}, \tag{23}$$

and $K = k\lambda_i$. The solution of (20) is

$$K^2 = \frac{R(2A - C) - \cos^2\alpha \pm \sqrt{\Delta}}{2M^2R^2}, \tag{24}$$

where

$$\Delta = \left[R(2A - C) - \cos^2\alpha\right]^2 - 4R^2A(A - C). \tag{25}$$

Linear (sinusoidal) waves correspond to $K^2 < 0$, while the reverse condition $K^2 > 0$ applies to exponentially varying nonlinear waves. A negative Δ corresponds to solutions which have complex wave numbers, i.e., nonlinear waves with oscillatory amplitudes. Such solutions have been previously identified in multi-ion plasmas and are called oscillitons [*Sauer et al.*, 2001, 2003; *Dubinin et al.*, 2003].

[15] In case of linear periodic waves, the Mach number $M = \omega/kV_A$ and frequency of small-amplitude waves in finite beta, anisotropic plasmas with ion and electron inertia can be expressed as

$$\frac{\omega^2}{\omega_{ci}^2} = K^2M^2, \tag{26}$$

which is a function of (M, α) parameterized by β, γ, κ, and a_p.

[16] If the electron inertia is neglected ($R\lambda^2{}_i = \lambda^2{}_e = 0$), equation (20) reduces to the dispersion equation for inertial ion waves [*Stasiewicz*, 2004a], which for isotropic ($a_p = 0$) and polytropic ($\kappa = 0$) plasma becomes

$$(k\lambda_i)^2 = \frac{\left(M^2 - \cos^2\alpha\right)^2}{M^2\cos^2\alpha}\left[\frac{2M^2\sin^2\alpha}{(2M^2 - \gamma\beta)(M^2 - \cos^2\alpha)} - 1\right]. \tag{27}$$

In the limit $k\lambda_i = 0$ this equation represents the Alfvén mode $M^2 = \cos^2\alpha$ and two magnetosonic modes

$$M_\pm^2 = \frac{1}{4}\left[2 + \gamma\beta \pm \left(4 + \gamma^2\beta^2 - 4\gamma\beta\cos 2\alpha\right)^{1/2}\right], \tag{28}$$

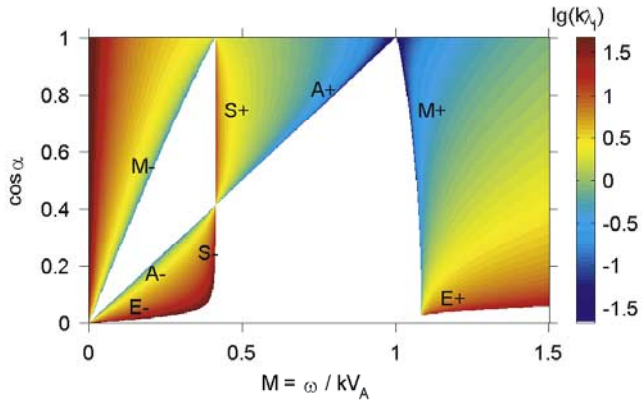

Figure 1. Phase portrait with wave numbers (color-coded) of linear MHD waves in a warm plasma ($\beta = 0.2$, $\gamma = 1.7$, $\kappa = 0$, $a_p = 0$) described by (24). There are eight modes of linear inertial waves grouped in four contiguous branches.

where $-$, $+$ denote slow and fast modes, respectively. Further simplification to a cold plasma ($\beta = 0$) yields

$$(k\lambda_i)^2 = -\frac{(M^2 - \cos^2\alpha)(M^2 - 1)}{M^2\cos^2\alpha}. \tag{29}$$

It is easily seen that for infinitely long wavelengths ($k\lambda_i \to 0$) we recover from (29) two ideal MHD modes [*Alfvén*, 1942]

$$\frac{\omega}{kV_A} = \cos\alpha, \tag{30}$$

$$\frac{\omega}{kV_A} = 1. \tag{31}$$

Naturally occurring Alfvén waves have finite wavelengths, and therefore terms containing $K = k\lambda_i$ generally must be retained. Because of the ordering of the dispersive scales for ions and electrons, $\lambda_i \gg \lambda_e$, the effects of the ion dispersion will always dominate the electron dispersion in modifying the propagation properties of hydromagnetic waves, except for the case of perpendicular propagation $\alpha \approx 90°$, which is seen in the left-hand sides of equations (9)–(10).

2.3. Waves in Warm Plasmas

[17] Figure 1 shows wave numbers (color-coded) of linear modes in a warm plasma described by equation (24) with $K^2 < 0$, $\Delta > 0$. The ion dispersion greatly enlarges the occurrence region for hydromagnetic waves, which cover a large area of the phase space. In warm plasmas defined by $m_e/m_i < \beta < 2/\gamma$ there are generally eight distinctively different linear modes: slow and fast Alfvénic (also called intermediate) waves (A_-, A_+), slow and fast magnetosonic waves (M_-, M_+) two ion-sound modes (S_-, S_+), which all depend on ion inertia, and additionally two electron inertia modes (E_-, E_+). The electron inertia effects are relevant only for shortest scales (dark red) near the axes of Figure 1. The most popular and best-known "shear Alfvén waves" occupy one point in Figure 1 ($M = 1$, $\cos\alpha = 1$) and represent limit $\lambda = \infty$.

[18] With use of equation (27), we can identify also the sonic shock line

$$M_{ss} = (\beta\gamma/2)^{1/2}, \tag{32}$$

which separates slow modes from fast modes, and the sonic angle

$$\cos\alpha_s = M_{ss}, \tag{33}$$

which separates Alfvén modes propagating subsonically and supersonically, or equivalently quasi-perpendicular ($q_\perp$) and quasi-parallel ($q_\parallel$) modes. More exactly, the sonic shock line corresponds to zero of the denominator in (23). Note that the sound speed is $V_s^2 = \gamma p_0/N_0 m_i = (\beta\gamma/2)V_A^2$ so that the Alfvén Mach number M_{ss} corresponds to the sonic Mach equal one. The S_+ modes move faster than the sound speed, while the S_- modes are slower than the sound speed. The divisions of the Alfvén and ion acoustic modes into two branches have not been well recognized in the literature.

[19] Historically, the linear Alfvén and magnetosonic modes are defined in the limit $k\lambda_i = 0$. The boundaries seen in Figure 1 correspond to this limit and show the Alfvén mode (30), two magnetosonic modes (28), and the sonic shock (32), with some modification due to electron inertia not included in these equations. It is seen, however, that topologically there are only four branches of linear waves in fluid formalism: (M_-), (A_+, S_+), (A_-, S_-, E_-), and (M_+, E_+). There is a continuous transition between the modes within each group, as the Mach number, propagation direction, wavelength, and wave frequency vary inside the group (see also Figure 6).

[20] In the gaps between the linear modes we find corresponding nonlinear waves ($K^2 > 0$) shown in Figure 2. While the linear waves behave $\propto \sin(kx)$ with constant amplitude, the nonlinear waves behave $\propto \exp(kx)$ at small amplitudes. As can be seen, the nonlinear waves occupy a large area of the phase space that is comparable in size to the area of the linear modes. To excite a nonlinear wave is as easy (or as difficult) as to excite a linear wave. One has to apply a perturbation to a specific point in the phase space (M, α). Topologically, there are only two branches of nonlinear modes, faster and slower than the Alfvén mode

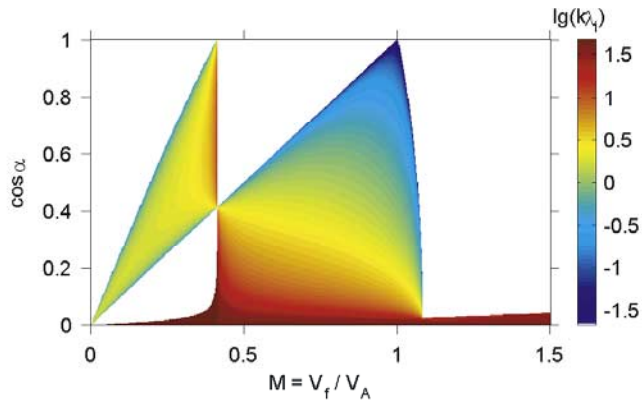

Figure 2. Nonlinear counterparts to linear waves shown in Figure 1. There are eight modes of nonlinear ion and electron inertial waves grouped in two contiguous branches. Color-coded is the exponential growth rate (24).

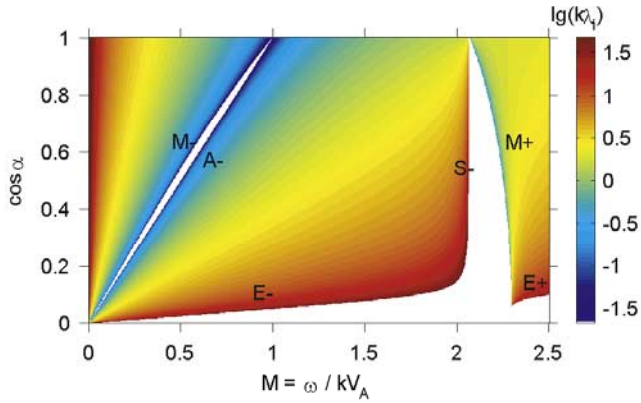

Figure 3. Phase portrait of linear waves in hot plasmas with $\beta = 5$, $\gamma = 1.7$, $\kappa = 0$, $a_p = 0$ described by equation (24). There are six modes of linear inertial waves in three branches.

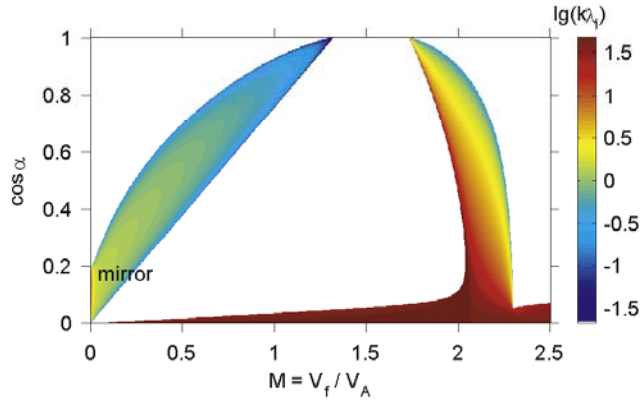

Figure 5. Same as Figure 4 but for anisotropic plasma with $a_p = -0.3$. Soliton solutions in the left corner correspond to "mirror-modes."

$V_A\cos\alpha$. However, through neighborhood to the linear modes of Figure 1, one can define eight corresponding nonlinear modes, (NM_-, NA_-, NS_-) in the slow branch and (NE_-, NS_+, NA_+, NM_+, NE_+) in the fast branch. The nonlinear Alfvén and sound modes are divided into two parts ($q_\perp$, $q_\parallel$) by the sonic angle (33) and by the sonic shock (32).

[21] In cold plasmas ($\beta < m_e/m_i$) the sonic shock line M_{ss} moves toward $M = 0$ and there are neither sound nor M_- waves but only one Alfvén branch (A_+) and the fast mode (M_+), as it is well known from linear theory. Hot plasma modes are shown in Figures 3 and 4. It can be seen that in a hot plasma, defined by $\beta > 2/\gamma$, there are three topologically different branches of linear waves (M_-), (A_-, S_-, E_-), and (M_+, E_+). The nonlinear waves in a hot plasma have two branches (NM_-, NA_-), and (NE_-, NS_+, NM_+, NE_+). The Alfvén and ion sound waves are no longer divided in two branches. The linear ion acoustic waves are below the sound speed, while the nonlinear ion acoustic waves are supersonic. Nonlinear fast-mode waves (NS_+, NM_+, E_+) in Figure 4 are observed by spacecraft at quasi-parallel Earth's bow shocks as large-amplitude shocklets with compressions of B and N by a factor of ten [*Stasiewicz et al.*, 2003a]. The fast magnetosonic shocklets exist in the literature under an ambiguous name of SLAMS, introduced by *Schwartz et al.* [1992]. The name is confusing because all nonlinear magnetic structures measured by spacecraft in the magnetosphere fall into the category of short large-amplitude magnetic structures (i.e., SLAMS). The physics of bow shocks (both $q_\parallel$ and $q_\perp$) pertains essentially to physics of fast electron and ion inertial nonlinear waves shown in Figures 4 and 5.

2.4. Mirror Modes

[22] The term "mirror modes" has been used in the literature to denote periodic magnetic pulsations with periods of 3–60 s (measured in satellite frame) and usually associated with large modulations of the magnetic field amplitude ($\delta B/B \sim \pm 80\%$) which have been measured by satellites in the magnetospheres of solar system planets and in the solar wind. In numerous experimental reports it has been established that these waves occur most commonly in regions of significant proton temperature anisotropy, $T_\perp > T_\parallel$, in a high-beta plasma, exhibit anticorrelations between magnetic field δB and density δN perturbations, have small velocity with respect to the plasma, and

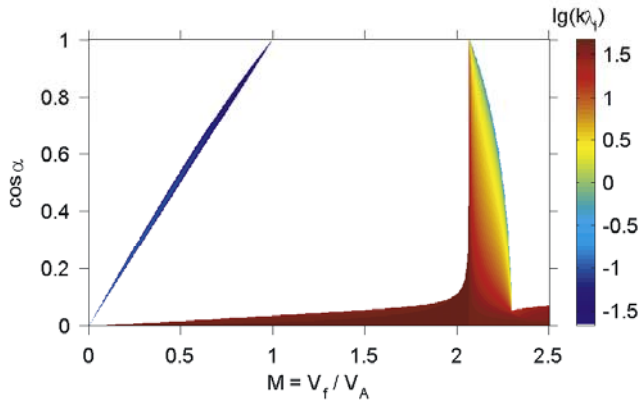

Figure 4. Nonlinear counterparts to linear waves shown in Figure 3. There are six modes of nonlinear waves in two branches.

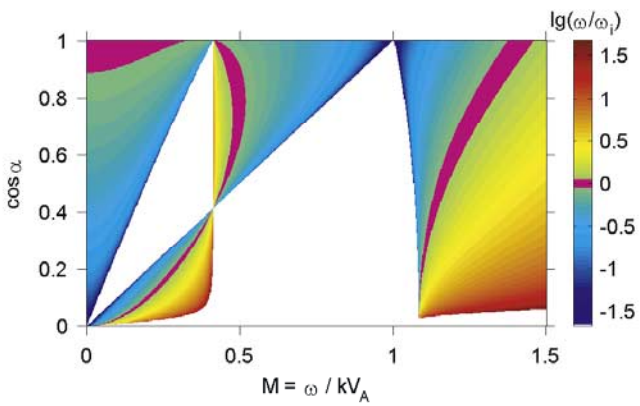

Figure 6. Frequency of linear waves from Figure 1. Color-coded is logarithm of (ω/ω_{ci}). Pink regions mark positions of the ion gyrofrequency.

Table 1. Effects of Varying Alfvén Speed on Linear Wave Modes Implied by Figures 1, 2, and 6[a]

$V_A(x)$ Decreasing ↙	Mode	Increasing $V_A(x)$ ↗
NS ←	M_-	→ short λ
short λ ← IC ←	A_-	→ NS
NS ←	E_-	
NS ←	LD ← S_- → LD	
	LD ← S_+ → LD	→ NS
NS ←	A_+	→ IC → short λ
IC ←	M_+	→ NS
NS ←	E_+	

[a]NS is nonlinear structure, IC is ion cyclotron, and LD is Landau damping.

propagate nearly perpendicular to **B**. Recently, *Stasiewicz* [2004b] has shown that all these properties correspond to nonlinear wave-train solutions from the left lower corner of Figure 4, i.e., to the branch of nonlinear waves identified as (NM_-, NA_-). In plasmas with perpendicular pressure anisotropy the region of nonlinear wave solutions is significantly enlarged (see Figure 5), which explains why these structures have been observed in mirror-mode stable (isotropic) plasmas, but their preferred location is a hot anisotropic plasma. It should be emphasized that there are no separate mirror modes either in the two-fluid, hot anisotropic plasma model or in the kinetic theory. Contrary to a popular belief, the paper by *Hasegawa* [1969] does not describe a new kinetic mirror mode but a purely growing instability, which in a fully nonlinear treatment corresponds to soliton solutions [*Stasiewicz*, 2004b].

2.5. Damping and Mode Conversion

[23] The fluid equations do not include either collisionless (Landau) damping of waves or ion cyclotron damping. It is known from kinetic theory that Landau damping maximizes in regions where the phase speed of waves is close to the thermal velocity of particles, while the cyclotron damping maximizes when the frequency of a wave is close to the gyrofrequency. The relevant ratio for the ion thermal velocity v_{ti}^2/V_f^2 equals β/M^2, and therefore Landau damping will maximize at $M \approx \sqrt{\beta} \approx M_{ss}$. As is well known, the damping is weak in plasmas with $T_e \gg T_i$, which places the sound speed above the ion and well below the electron thermal speed. The expected ion cyclotron damping can be located with help of Figure 6, which shows the frequency of linear waves described by (26). The pink band marks regions around the ion gyrofrequency, where damping/interactions with ion cyclotron waves are expected.

[24] There are strong gradients in the Alfvén speed in the magnetosphere because of variations of both magnetic field and plasma density. A small-amplitude wave launched at a specific location with (ω, k, cosα), propagating in a medium with varying $V_A(x)$, will have varying Mach number $M(x) = \omega/kV_A(x)$, and may become nonlinear as it tunnels from linear regions in Figure 1 to the nonlinear regions depicted in Figure 2. Generally, a linear wave may become nonlinear (i.e., move from Figure 1 to Figure 2) through variations of any of the parameters, α(x), β(x), $M(x)$, which enter the governing equations. Variations of α(x) may be caused by changes of the magnetic field direction or the ray path in inhomogeneous medium. A variation of β results in the movement of the vertical sound line (32) from $M \approx 0$ for a cold plasma to $M \approx 2$ for the presented hot plasma case. Unless $\beta_e \gg \beta_i$, we should have the sonic shock line (32) playing the role of a dissipation layer for fast waves (A_+) moving in a medium with increasing V_A and for slow waves (A_-) propagating in a medium with decreasing V_A. Table 1 summarizes effects associated with propagation of different modes in a medium with varying Alfvén speed, compiled on the basis of Figures 1, 2, and 6.

3. Nonlinear Solutions

[25] The previous analysis concerned the dispersion relations based on a linearized set of equations. It was useful to determine the location of different modes in the phase space (M, α) and to determine the locations of linear and nonlinear solutions. This linear analysis can identify locations of exponentially varying solutions but cannot predict the evolution of nonlinear waves. This must be done in a case by case basis through numerical integration of the fully nonlinear set of equations. The integration shows that the growth of nonlinear waves can either be balanced by dispersive effects or not. In the first case, the nonlinear wave is a stationary wave and represents a soliton or a cnoidal wave. If the exponential growth is not balanced by dispersive effects, equations (9)–(10) have divergent numerical solutions, which means that such a wave is not stationary and must be described by an explicitly time-dependent model. Eventually, it would break down and dissipate its energy in a manner similar to ocean waves which steepen and dissipate in front of a beach.

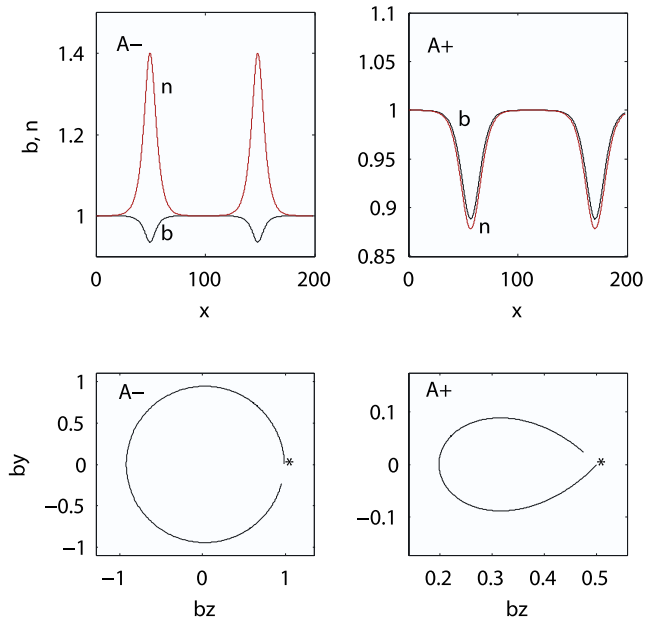

Figure 7. Exact solutions of nonlinear Alfvén waves for parameter range from Figure 2, slow Alfvén, (NA_-) for α = 80°, M = 0.1731 and fast Alfvén (NA_+) for α = 30°, M = 0.946. The NA_- wave is left-handed and NA_+ is right-handed (asterisks mark start points of the hodograms). The b_x axis is into the plane of the figure. The x axis is in units of λ_i and the magnetic field and the density are shown in normalized units.

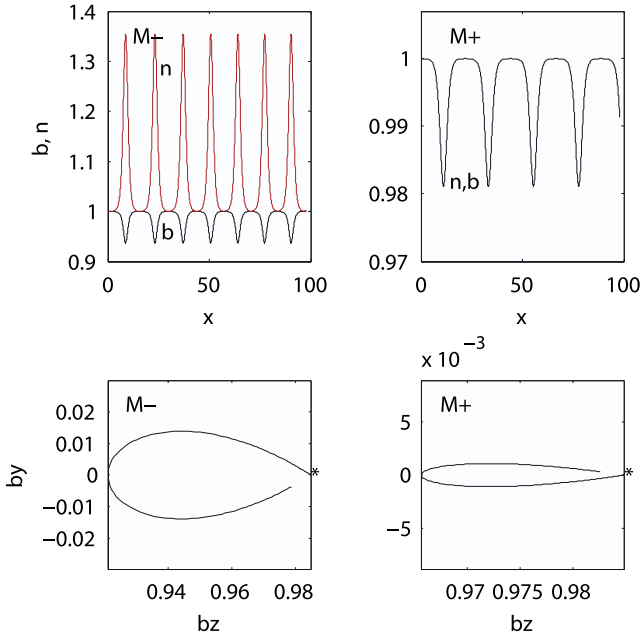

Figure 8. Amplitudes and polarizations of nonlinear magnetosonic waves, slow (NM_-) for $\alpha = 80°$, $M = 0.0746$ and fast (NM_+) for $\alpha = 80°$, $M = 1.0651$. The density variation overlap the magnetic field variation for NM_+. Plasma parameters are as in Figure 7.

[26] We now proceed to the investigation of properties of nonlinear waves described by the full set of equations (8)–(18). It is not possible to provide the general characteristic of nonlinear solutions because it would require numerical integration for each point in the phase space. Examples of stationary nonlinear wave solutions are shown in Figure 7 (Alfvén modes), Figure 8 (magnetosonic modes), and Figure 9 (sound waves). Polarization of the transverse

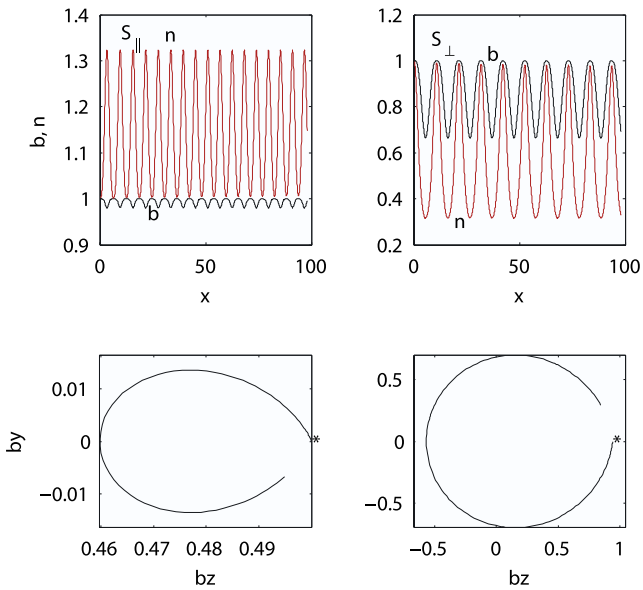

Figure 9. Amplitudes and polarizations of nonlinear ion sound waves, (NS_+) for $\alpha = 30°$, $M = 0.39$ and (NS_-) for $\alpha = 70°$, $M = 0.41$. Plasma parameters are as in Figure 7.

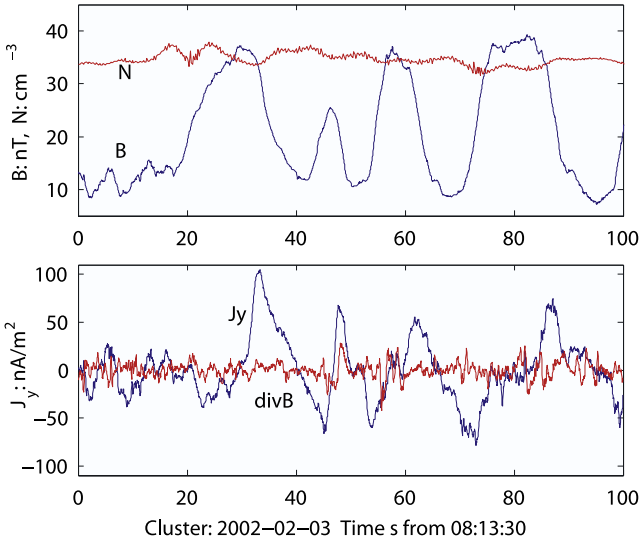

Figure 10. Cluster measurements of trains of solitons in the magnetosheath. (top) Total magnetic field and electron density from spacecraft C1. (bottom) The dominant current J_y component determined from $\mu_0^{-1}\nabla \times \mathbf{B}$ and $\mu_0^{-1}\nabla \cdot \mathbf{B}$ in current units as a measure of the accuracy of the analysis. Solitary structures are built of current sheets with opposite directions.

components of the magnetic field is also displayed. It can be seen that the modes slower than the sound speed have left-handed polarization, while the faster modes are right-handed.

[27] As discussed by *Stasiewicz* [2004a, 2004b] any nonlinear solution, depending on the initial perturbation, can proceed from $n = 1$, $b = 1$ to a new state, either with increased density and magnetic field ($\delta n+$, $\delta b+$) or to other possible combinations ($\delta n-$, $\delta b-$), ($\delta n+$, $\delta b-$), ($\delta n-$, $\delta b+$), along the $b(n)$ dependence described by the momentum conservation (8). For wave speeds faster than the ion sound speed ($M > M_{ss}$) only in-phase solutions ($\delta n/\delta b > 0$) are possible, while structures moving slower than sound ($M <$

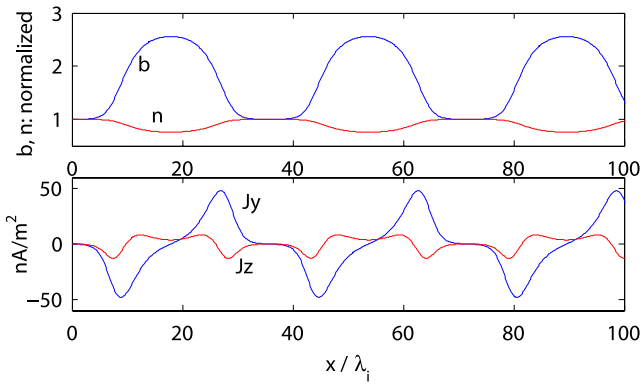

Figure 11. Exact solutions of (8)–(10) for $\beta = 15$, $M = 0.07$, $\gamma = 1.7$, $a_p = 0.1$, $\alpha = 83.8$. (top) Total magnetic field and electron density in normalized units. (bottom) The computed current J_y and J_z in physical units ($J_x \equiv 0$). Distance of 100 λ_i corresponds to approximately 50 s in Figure 10.

M_{ss}) can only have off-phase solutions ($\delta n/\delta b < 0$). To achieve a soliton train solution, there must be a balance between the nonlinear growth rate and dispersion in equations (9)–(10). For given plasma parameters, such a balance can be achieved only for some combinations of ($\delta n\pm$, $\delta b\pm$).

[28] There are no damping mechanisms in the model, and all solutions conserve momentum and energy. The total energy content given by the sum of all four components in equation (8) is strictly preserved along the integration path x in all numerical solutions shown in this paper. The nonlinear structures are produced by exchange between dynamic, thermal energy of plasma and the magnetic field energy in a way prescribed by the equations of state and momentum conservation.

4. Comparison With Measurements

[29] The applicability of fluid equations to finite-β plasmas has been debated in the literature. The reader may ask the legitimate question how relevant the presented theory is for the description of phenomena in real plasmas. We believe that this question should be answered by comparing predictions of the theory with experimental results. It has been demonstrated previously [*Stasiewicz et al.*, 2003b; *Stasiewicz*, 2004a, 2004b] that solutions of equations (8)–(10) in the limit $R = 0$ (without electron inertia) provide realistic solutions to solitons and mirror modes observed by Cluster in the magnetosheath and in the boundary layer for plasma beta range 0.1–10. Below we provide additional evidence for the applicability of the presented model to high-beta plasmas by comparing electric currents measured by Cluster (Figure 10) with currents computed from the model using equations (8)–(15) and shown in Figure 11. This case pertains to a hot ($\beta \approx 15$), anisotropic plasma ($T_\perp/T_\parallel \approx 1.2$) with the phase space portrait similar to that shown in Figure 5.

[30] The current determined from Cluster data is computed directly as $\mu_0^{-1}\nabla \times \mathbf{B}$ with use of measurements from the four spacecraft separated ~100–200 km apart. The accuracy of current determination is checked by computing $\mu_0^{-1}\nabla \cdot \mathbf{B}$ which is also shown in Figure 10. The current components J_x, J_z determined from Cluster are not displayed here because they are comparable to the error level given by the divergence of measured B. It can be seen in Cluster measurements that solitons (''mirror modes with peaks'') correspond to sheets of oppositely directed currents. The current determined from the model (Figure 11) is expressed in physical units using the normalization $B_0/\mu_0\lambda_i$ with $B_0 = 10$ nT and $\lambda_i = 40$ km, taken from the case published by *Stasiewicz* [2004a, 2004b]. The plasma structures move over the spacecraft with speeds of 100 km/s, which is equivalent to 2 λ_i/s. This means that 1 s of Cluster data corresponds to ~2λ_i in computations. As can be seen in Figure 11, the current derived from the model is in good quantitative agreement with the current determined with Cluster measurements and that the model reproduces well both the amplitude and the structure of the measured currents and size of the solitons.

5. Conclusions

[31] We have presented a general overview of linear and nonlinear magnetohydrodynamic waves in a wide range of plasma beta ($0 < \beta < 15$) in anisotropic plasmas with both ion and electron inertia effects. We have found eight linear (sinusoidal) and eight nonlinear (cnoidal) wave modes in a warm plasma ($m_e/m_i < \beta < 2/\gamma$). These waves are identified as slow and fast Alfvén (A_-, A_+), slow and fast magnetosonic (M_-, M_+), ion sound modes (S_-, S_+), and electron inertial waves (E_-, E_+). Topologically, they form four contiguous branches of linear waves (M_-), (A_+, S_+), (A_-, S_-, E_-), (M_+, E_+), and two contiguous branches of nonlinear waves (NM_-, NA_-, NS_-), (NE_-, NS_+, NA_+, NM_+, NE_+). The dispersive properties of linear and nonlinear waves and their wavelengths and frequencies are presented in a novel way as portraits in the (M, α) phase space. Inclusion of electron inertia modifies the dispersion patterns near $\alpha \approx 90°$, introducing the electron modes, that will be analyzed in a separate publication. Except for electron inertial waves, all other modes depend strongly on the ion inertial length λ_i. The wave modes described in this paper, $A_\pm$, $M_\pm$, $S_\pm$, both linear and nonlinear, represent ion inertial waves, which become electron inertial waves ($E_\pm$) at the critical propagation angle $\cos\alpha_I \sim M(m_e/m_i)$, implied by equations (9)–(10).

[32] It is shown how the phase portrait of these waves changes at the transition between warm and hot plasmas ($\beta \approx 1$) and how trains of solitons are produced in a hot, anisotropic plasma. It is pointed out that there are no separate mirror modes in the fluid formalism, but an anisotropic plasma pressure enhances greatly the occurrence area of soliton trains (cnoidal waves), which represent a mathematical model for structures that have been described as ''mirror-mode waves'' by experimentalists. Furthermore, it is argued that the physics of bow shocks (both $q_\parallel$ and $q_\perp$) pertains essentially to physics of fast electron and ion inertial waves (NS_+, NM_+, NE_+) shown in Figures 4 and 5. The terminology of SLAMS (short large-amplitude magnetic structures) used in this context is confusing because all nonlinear magnetic structures measured by satellites in the magnetosphere (including small-scale auroral structures) would fall into this category.

[33] It is also shown that the nonlinear modes slower than the ion sound speed have left-handed polarization for the transverse magnetic field, while the faster modes have right-handed polarization. The applicability of the model is illustrated by showing that the electric currents carried by nonlinear waves measured on Cluster spacecraft in the magnetosheath at $\beta \approx 15$ are well reproduced by currents derived from the theoretical model.

[34] The results of this paper provide a simple and transparent method for identification of linear and nonlinear magnetohydrodynamic waves using only the propagation direction α (determined from the minimum variance analysis of **B**), phase speed $M = \omega/kV_A$, signature of $\delta B/\delta N$, and/or polarization of the transverse magnetic field.

[35] **Acknowledgment.** Shadia Rifai Habbal thanks Youra Taroyan and Roberus von Fay-Siebenburgen for their assistance in evaluating this paper.

References

Alfvén, H. (1942), Existence of electromagnetic-hydromagnetic waves, *Nature*, *150*(3805), 405–406.

Anderson, B. J., S. A. Fuselier, S. P. Gary, and R. E. Denton (1994), Magnetic spectral signatures in the Earth's magnetosheath and plasma depletion layer, *J. Geophys. Res.*, *99*, 5877.

Baumgärtel, K. (1999), Soliton approach to magnetic holes, *J. Geophys. Res.*, *104*, 28,295.

Braginski, S. I. (1965), Transport processes in a plasma, in *Reviews of Plasma Physics*, vol. 1, edited by M. A. Leontovich, p. 205, Consultants Bureau, New York.

Denton, R. E., X. Li, and T.-D. Phan (1995), Bounded anisotropy fluid model for ion temperature evolution applied to AMPTE/IRM magnetosheath data, *J. Geophys. Res.*, *100*, 14,925.

Dubinin, E., K. Sauer, J. F. McKenzie, and G. Chanteur (2003), Solitons, oscillitons, and stationary waves in a warm p-alpha plasma, *J. Geophys. Res.*, *108*(A7), 1296, doi:10.1029/2002JA009572.

Formisano, V., and C. F. Kennel (1969), Small amplitude waves in high beta plasmas, *J. Plasma Phys.*, *3*, 55.

Gary, S. P., B. J. A. R. E. Denton, S. A. Fuselier, and M. E. McKean (1994), A closure relation for anisotropic plasmas from the Earth's magnetosheath, *Phys. Plasmas*, *1*, 1676.

Gekelman, W., S. Vincena, N. Palmer, P. Pribyl, D. Leneman, C. Mitchell, and J. Maggs (2000), Experimental measurements of the propagation of large-amplitude shear Alfvén waves, *Plasma Phys. Contr. Fusion*, *42*(12) suppl. B, B15–B26.

Goertz, C. K., and R. W. Boswell (1979), Magnetosphere-ionosphere coupling, *J. Geophys. Res.*, *84*, 7239–7246.

Hasegawa, A. (1969), Drift mirror instability in the magnetosphere, *Phys. Fluids*, *12*, 2642.

Hasegawa, A. (1976), Particle acceleration by MHD surface wave and formation of aurora, *J. Geophys. Res.*, *81*, 5083–5090.

Hau, L. N., and B. U. Ø. Sonnerup (1991), Self-consistent gyroviscous fluid model of rotational discontinuities, *J. Geophys. Res.*, *96*, 15,767.

McKenzie, J. F., E. Dubinin, K. Sauer, and T. B. Doyle (2003), The applications of the constants of motion to nonlinear stationary waves in complex plasmas: A unified fluid dynamic viewpoint, *J. Plasma Phys.*, *70*, 1–32.

Sauer, K., E. Dubinin, and J. McKenzie (2001), New type of soliton in bi-ion plasmas and possible implications, *Geophys. Res. Lett.*, *28*(18), 3589.

Sauer, K., E. Dubinin, and J. McKenzie (2003), Solitons and oscillitons in multi-ion space plasmas, *Nonlinear Proc. Geophys.*, *10*, 121.

Schwartz, S. J., D. Burgess, W. P. Wilkinson, R. L. Kessel, M. Dunlop, and H. Lühr (1992), Observations of short large-amplitude magnetic structures at a quasi-parallel shock, *J. Geophys. Res.*, *97*(A4), 4209.

Stasiewicz, K. (2004a), Theory and observations of slow-mode solitons in space plasmas, *Phys. Rev. Lett.*, *93*(12), 125004, doi:10.1103/PhysRevLett.93.125004.

Stasiewicz, K. (2004b), Reinterpretation of mirror modes as trains of slow magnetosonic solitons, *Geophys. Res. Lett.*, *31*, L21804, doi:10.1029/2004GL021282.

Stasiewicz, K., et al. (2000), Small scale Alfvénic structure in the aurora, *Space Sci. Rev.*, *92*(3-4), 423–533.

Stasiewicz, K., M. Longmore, S. Buchert, P. Shukla, B. Lavraud, and J. Pickett (2003a), Properties of fast magnetosonic shocklets at the bow shock, *Geophys. Res. Lett.*, *30*(24), 2241, doi:10.1029/2003GL017971.

Stasiewicz, K., P. K. Shukla, G. Gustafsson, S. Buchert, B. Lavraud, B. Thide, and Z. Klos (2003b), Slow magnetosonic solitons detected by the Cluster spacecraft, *Phys. Rev. Lett.*, *90*(8), 085002, doi:10.1103/PhysRevLett.90.085002.

Stefant, J. R. (1970), Alfvén wave damping from finite gyroradius coupling to the ion acoustic mode, *Phys. Fluids*, *13*, 440.

Stringer, T. E. (1963), Low-frequency waves in an unbounded plasma, *Plasma Phys.*, *5*, 89–107.

Vincena, S., W. Gekelman, and J. Maggs (2004), Shear Alfvén wave perpendicular propagation from the kinetic to the inertial regime, *Phys. Rev. Lett.*, *93*(10), 105003, doi:10.1103/PhysRevLett93.105003.

K. Stasiewicz, Swedish Institute of Space Physics, Box 537, SE-751 21 Uppsala, Sweden. (k.stasiewicz@irfu.se)